Sand displacement field analysis during pile installation using x-ray tomography and digital image correlation

M. Silva & G. Combe
Université Grenoble Alpes, 3SR, F-38000, Grenoble, France
CNRS, 3SR, F-38000, Grenoble, France

ABSTRACT: This article presents the results of a 5.5 mm model pile installation on a silica sand sample under isotropic confinement by using X-ray microtomography and three dimensional Digital Image Correlation on a model calibration chamber. The incremental sand displacement field was calculated during the pile installation both locally around the pile tip and for the entire volume. Displacement vectors and normalized strain contours are obtained for each incremental loading step. Evidence of sand flows near the pile tip gives new ideas about the possible mechanisms controlling the lateral friction of piles.

1 INTRODUCTION

The kinematics behind the installation of driven piles in silica sand remains an area of great uncertainties. Most of the shear capacity of a driven pile takes place on a thin layer of sand in contact with the pile's surface. Several authors have suggested that the time dependent behaviour of this sand layer and possible sand arching effects generated during pile installation would control the long term capacity of driven piles in sand and probably explain the phenomenon of lateral friction set-up, Åstedt et al. (1992), Chow et al. (1998), Axelsson (2000). It is then essential to understand the interaction between the pile and the surrounding soil.

Robinsky & Morrison (1964) using x-ray radiographies during the installation of a model pile concluded that a zone of loose sand will form around the pile during its installation. The sand near the pile's surface is dragged down with the pile movement under the constant confinement of the surrounding soil resulting in the formation of an arc of sand around the pile. Chong (1998) from density measures on large calibration chamber tests, Allersma (1988) and Allersma et al. (2002) from photoelastic observations on a plain strain model, and Van Nes (2004), Ngan-Tillard et al. (2005) and Morita et al. (2007) using x-ray tomography on small laboratory samples have confirmed the presence of a layer of loose sand around the shaft.

White and Bolton (2002) and White and Bolton (2004) using Particle Image Velocimetry (PIV) on a plain strain model suggested that a zone of high density will develop around the pile as the latter embeds deeper into the sand mass. Their results show irrecoverable volume reduction beneath the pile tip resulting from particle breakage and soil compaction. As the pile embeds into this highly overconsolidated sand, a zone of high density will be created around the shaft. White and Bolton suggested that with continuing pile installation the cylindrical cavity of the stiff overconsolidated sand will collapse leading to a reduction in radial stress and to a similar arching phenomenon as the one presented by Robinsky & Morrison (1964). The number of shearing cycles during installation plays a crucial role when comparing results from monotonic and pseudo-dynamic installation, White and Lehane (2004). Yang et al. (2010) reported the presence of a thin layer of compacted broken grains with high particle interlocking around a cyclically jacked model pile

Allersma (1988) observed high stress concentration beneath the pile when embedding in the soil with rotation of principal stresses with the principal stress perpendicular to the tip edge. Recently Jardine et al. (2013) interpreted the sand stress field during the installation of model pile into a pressurized calibration chamber. Their results show similar stress distributions as those suggested by White and Bolton (2004).

This paper presents the first results of an experimental programme devoted to the analysis of the displacement field developed after the installation of a model pile into a silica sand sample in a model calibration chamber using micro tomography (x-ray micro CT) and three dimensional (3D) digital image correlation (DIC).

2 EXPERIMENTAL ARRANGEMENTS

The tests were conducted in the micro CT tomograph of the laboratory 3SR in Grenoble, France. An un-instrumented 5 mm diameter (*B*) cone ended aluminum model pile was installed by monotonic loading on a dry silica sand sample under an isotropic confinement pressure.

The sample consists of a 70 mm diameter (*D*), 100 mm height of Fontainebleau NE34 silica sand. Bolton et al. (1999) concluded from centrifuge tests on model piles with this sand, that the minimum distance between the pile and any hard boundary (*D/B*) should be at least 10, and that the ratio between pile diameter and the mean particle size (B/d_{50}) should be at least 20. In our case the ratio *D/B* and B/d_{50} are 14 and 23 respectively. Sample size and mean grain size are restricted by the scanning conditions during x-ray micro CT. Possible scale effects are expected in the results.

Table 1: Index properties of Fontainebleau NE34 sand

e_{min}	e_{max}	d_{10} (mm)	d_{50} (mm)	d_{60} (mm)
0.51	0.90	0.15	0.21	0.23

Samples were prepared by four consecutive layers of 25 mm height and a density of 1.60 gr/cm^3, corresponding to a relative density of approx. 70%. A constant isotropic confinement pressure of 100 kPa was applied during pile installation and scanning.

For practical reasons, the pile was installed from the bottom of the cell monotonically 50 mm into the sand mass at a rate of 0.1 mm/s where a first tomogram was obtained. The pile head load was kept constant during the different tests.

Several tomograms were then obtained after incremental pile displacements ranging from 0.5 to 2.0 mm, in order to perform further digital image correlation analyses to evaluate the incremental displacement field between consecutive loading steps.

The general arrangements for the tests are presented in figure 1.

3 X-RAY MICRO CT AND 3D-DIC

The pile penetration was done progressively, stopping penetration at defined intervals for 3D scanning. Scans were settled to a tension of 200kV and a current of 150 μA. 1024 radiographies were made of the sand samples for the reconstruction of the entire volume. Using micro CT, a 3D digital image of the x-ray attenuation in the soil sample and the pile was obtained. Two different distances from the x-ray source were considered in order to perform a global and local tomography, which allow focusing on precise zones inside the sample. A resolution of approx. 23 and 43 μm/pixel were obtained for global and local tomography respectively.

An example of the reconstructed volume during a local tomography is presented in figure 2.

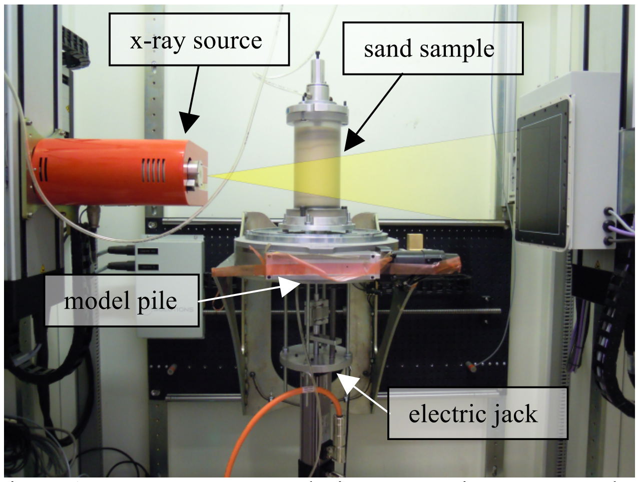

Figure 1: Test arrangements during x-ray micro tomography.

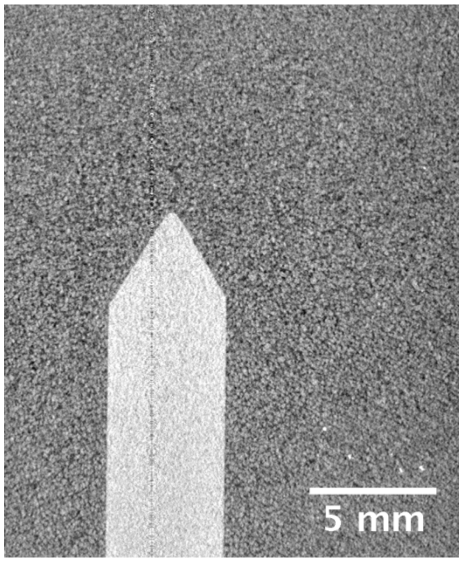

Figure 2: Vertical slice across the sand sample during local tomography.

The spatial deformation between two consecutive x-ray tomograms was mapped and analyzed by applying 3D-DIC, which compares the texture of character between a predefined volume sample. For the results here presented a 14 pixels side cube was considered.

The full strain tensor field in the form of volumetric strain and maximum shear (distortional) strains was derived using the 3D-DIC code TomoWarp (Hall, 2006; Hall et al., 2010). This code calculates the strains from the derived displacements under continuum assumptions.

Similar techniques were recently used by Paniagua et al. (2013) for the analyses of a penetrating CPT in silts.

4 RESULTS

Typical results from an incremental pile displacement are presented in figures 3 and 4. Displacement contours are plotted in the vertical and horizontal axis at normalized distances from the pile axis, *h/r*, where *h* is the distance from the pile axis, and *r* the pile radius.

The results show two distinct areas of particle movements. The first zone, which concentrates most of the movements, is observed beneath the pile tip. The sand particles follow the pile movement in the vertical direction and spread horizontally perpendicularly to the cone ended tip angle, at approx. 60°. Most of the particle displacements are concentrated in a region up to a distance of approx. 1 pile diameter beneath the tip.

A second characteristic area with lower displacement locates behind the tip pile. In this region a thin layer of sand follows the movement of the pile in the vertical direction, whereas the surrounding soil is shows evidence of particle recirculation. Figure 6 shows two dimensional representations of displacement vectors in this area. The displacement field was calculated every 4 pixels. These observations are similar to those obtained by Pater & Nieuwenhuis (1986) using photographic techniques. As the pile movement progresses, sand particles are moved upward in the opposite direction of the pile movement, and against the pile by the surrounding soil. This particle recirculation seems consistent with the radial stress reduction in the soils stresses measured by Jardine et al. (2013).

As presented in Figure 6, the magnitude of the displacement in the area where recirculation takes place is significantly lower than beneath the pile tip. Analyses continue to evaluate the effects of confining pressure, imposed pile displacement and mean particle size.

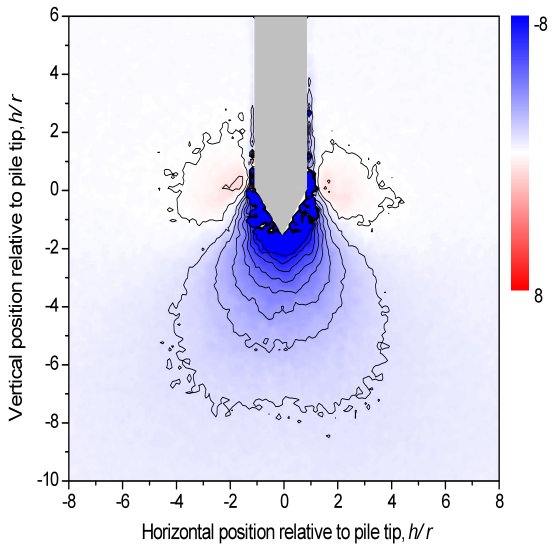

Figure 3: Incremental displacement along Y-axis after a 2 mm pile head displacement (values in pixel, 1 pixel = 43 µm).

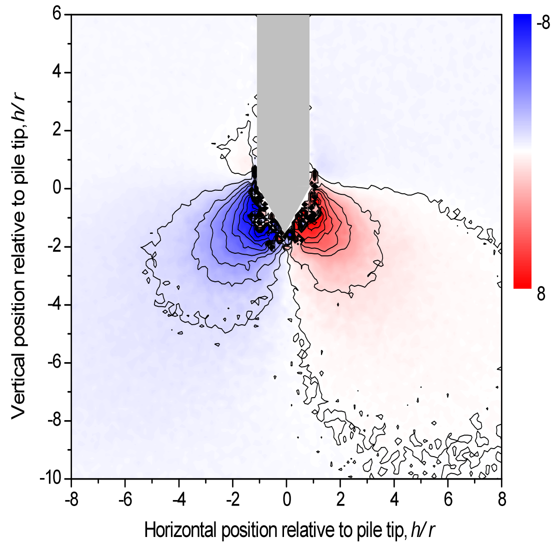

Figure 4: Incremental displacement along vertical axis after a 2 mm pile head displacement (values in pixel, 1 pixel = 43 µm).

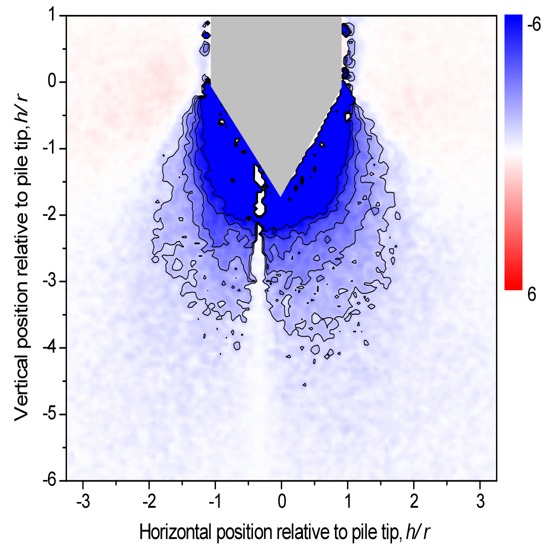

Figure 5: Incremental displacement along vertical axis after a 2 mm pile head displacement (values in pixel, 1 pixel = 23 µm).

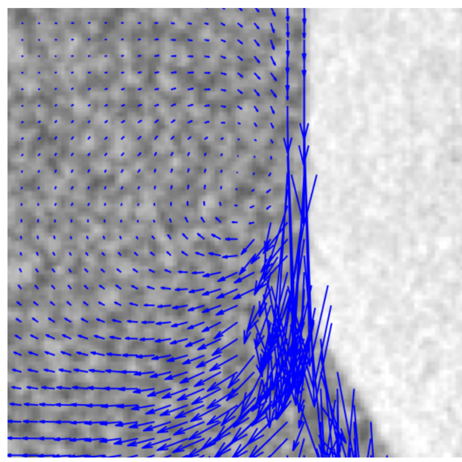

Figure 6: Two dimensional displacement vectors around the pile tip after a 2 mm pile head displacement. Vectors are amplified by a factor 10.

The analysis of strain patterns during a loading step can be characterized by figures 7 and 8. The main strains develop mostly around and beneath the pile tip. A zone of high vertical contraction and horizontal extension develops beneath the pile tip as the pile is continuously pushed into the sand. Behind this zone and almost perpendicular to the cone tip edge, a zone of vertical extension and horizontal compression will develop. These results confirm White and Bolton (2004) findings from PIV tests on plain strain models.

The interaction between these two zones would explain the recirculation of sand particles presented in figure 6. As the pile is installed into the sand mass, highly compacted sand particles from beneath the pile tip are pushed radially upwards with the tip movement, and compressed against the pile surface by the surrounding soil.

Figures 9 and 10 show a comparison between the shear strain developed between two different steps of 0.5 and 2 mm. Shear strain concentrate locally around the tip and as the displacement steps increase, the area of influence becomes more important and expands to the pile's shaft.

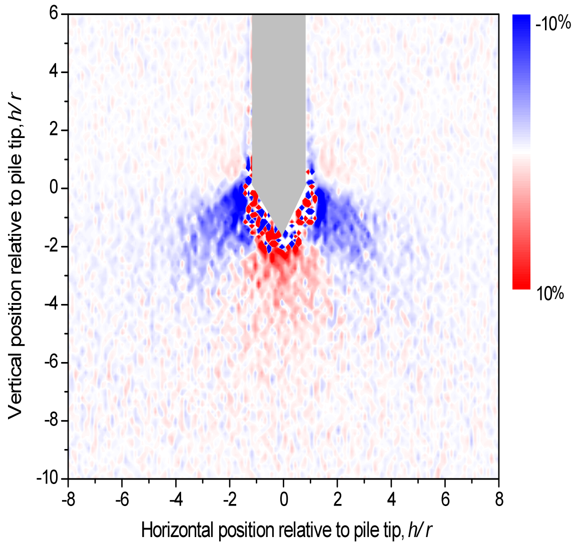

Figure 7: Incremental horizontal strain after a 2 mm pile head displacement.

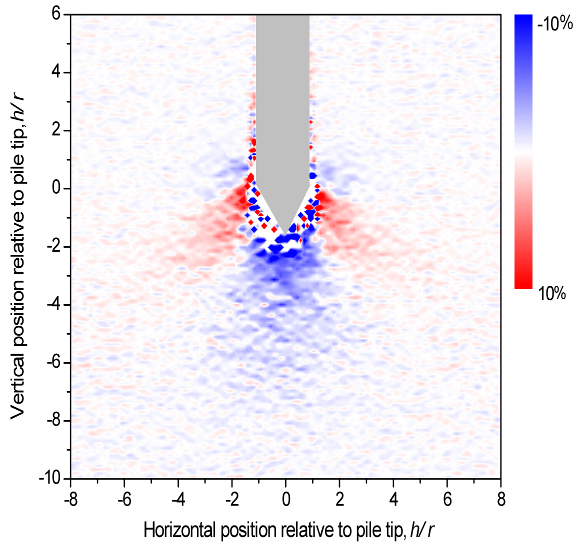

Figure 8: Incremental vertical strain after a 2 mm pile head displacement.

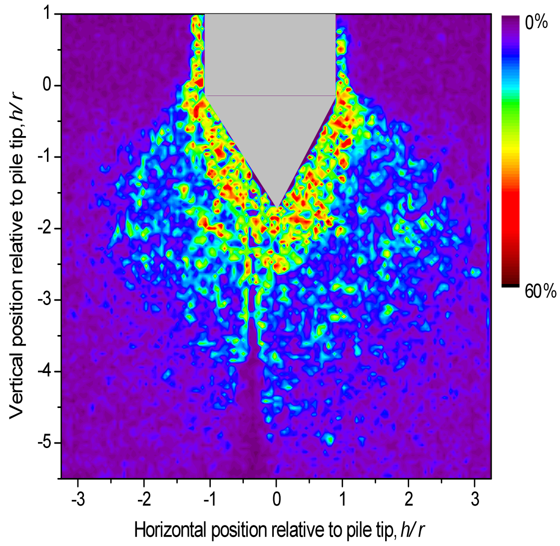

Figure 9: Incremental shear strain after a 0,5 mm pile head displacement. Local tomography.

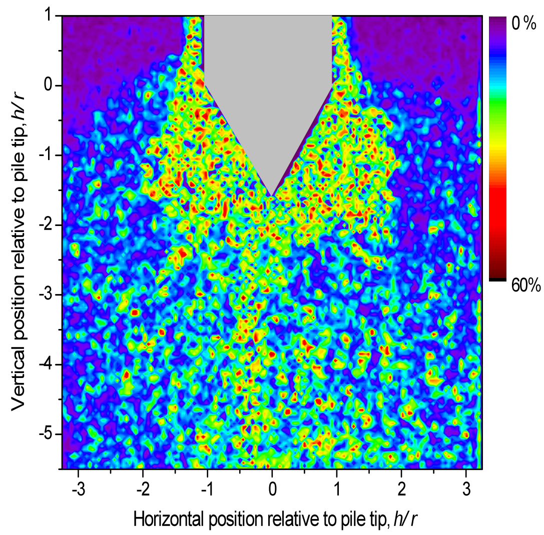

Figure 10: Incremental shear strain after a 2 mm pile head displacement. Local tomography.

CONCLUSIONS

The combined use of x-ray micro CT with 3D-DIC allows understanding the kinematics behind the installation of a geotechnical probe on a silica sand sample. Different zones of influence for the vertical and horizontal strains were identified. The results suggest the presence of a zone behind the pile tip where recirculation of sand particles takes place.

REFERENCES

Åstedt, B., Weiner, L., & Holm, G. (1992). Increase in bearing capacity with time for friction piles in silt and sand. *Proceedings of Nordic Geotechnical Meeting*, 411-416.

Allersma, H. G. B. (1988). Optical analysis of stress and strain around the tip of a penetrating probe. *Penetration Testing 1988*, Vol. 2, 615–620, Balkema, Rotterdam.

Allersma, H., & Broere, W. (2002). Optical analysis of stress around a penetrating probe in granular material. *Physical modelling in geotechnics: proceedings of the international conference on physical modelling in geotechnics*, 149–154.

Axelsson, G. (2000). Long-Term Set-Up of Driven Piles in Sand. Phd Thesis, Royal Institute of Technology, Sweden.

Bolton, M. D., Gui, M. W., Garnier, J., Corte, J. F., Bagge, G., Laue, J., & Renzi, R. (1999). Centrifuge cone penetration tests in sand. *Géotechnique*, 49(4), 543–552.

Chong, M. K. (1988). Density changes of sand on cone penetration resistance. *Penetration Testing 1988*, Vol. 2, 707–714, Balkema, Rotterdam.

Chow, F. C., Jardine, R. J., Brucy, F., & Nauroy, J. F. (1998). Effects of Time on Capacity of Pipe Piles in Dense Marine Sand. *Journal of Geotechnical and Geoenvironmental Engineering*, 124(3), 254-264.

Hall, S. A. (2006). A methodology for 7D warping and deformation monitoring using time-lapse seismic data. *Geophysics*, 71(4), O21-O31.

Hall, S. A., Bornert, M., Desrues, J., Pannier, Y., Lenoir, N., Viggiani, G., & Besuelle, P. (2010). Discrete and continuum analysis of localised deformation in sand using X-ray uCT and volumetric digital image correlation. *Geotechnique*, 60(5), 315–322.

Jardine, R., Zhu, B., Foray, P., & Yang, Z. (2013). Interpretation of stress measurements made around closed-ended displacement piles in sand. *Geotechnique*, 63(8), 613–627.

Morita, K., Otani, J., Mukunoki, T., Hironaka, J., & Pham, K. D. (2007). Evaluation of vertical and lateral bearing capacity mechanisms of pile foundations using X-ray CT. *Advances in Deep Foundations: International Workshop on Recent Advances of Deep Foundations*, 217–223, Taylor & Francis.

Ngan-Tillard, D., Cheng, X. H., Van Ness, J., & Zitha, P. L. J. (2005). Application of x-ray computed tomography to cone penetration tests in sands. *Proceedings of the Geo-Frontiers, Site Characterization and Modeling*, 1–12.

Paniagua, P., Andò, E., Silva, M., Emdal, A., Nordal, S., & Viggiani, G. (2013). Soil deformation around a penetrating cone in silt. *Géotechnique Letters*, 3, 185–191.

Pater, C. De, & Nieuwenhuis, J. (1986). Method for measuring the deformations of a sand surface. *Geotechnique*, 36(4), 581-585

Robinsky, E. I., & Morrison, C. (1964). Sand displacement and compaction around model friction piles. *Canadian Geotechnical Journal*, 1(2), 81–93.

Van Nes, J. H. . (2004). Application of computerized tomography to investigate strain fields caused by cone penetration in sand. (Master's thesis). Delft University of Technology.

White, D., & Bolton, M. (2002). Observing friction fatigue on a jacked pile. *Centrifuge and Constitutive Modelling: Two extremes*, 347-354.

White, D. J., & Bolton, M. D. (2004). Displacement and strain paths during plane-strain model pile installation in sand. *Géotechnique*, 54(6), 375–397.

White, D. J. D., & Lehane, B. M. B. (2004). Friction fatigue on displacement piles in sand. *Géotechnique*, 54(10), 645–658.

Yang, Z. X., Jardine, R. J., Zhu, B. T., Foray, P., & Tsuha, C. H. C. (2010). Sand grain crushing and interface shearing during displacement pile installation in sand. *Géotechnique*, 60(6), 469–482.